Articles

The Unfolding of *trp* Aporepressor as a Function of pH: Evidence for an Unfolding Intermediate†

Maurice R. Eftink,* Kathy J. Helton, Antonia Beavers, and Glen D. Ramsay

Department of Chemistry, University of Mississippi, University, Mississippi 38677

Received March 29, 1994; Revised Manuscript Received June 24, 1994®

ABSTRACT: The urea-induced unfolding of *trp* aporepressor from *Escherichia coli* has been studied as a function of pH from 2.5 to 12.0 at 25 °C. At pH 7 and above, the unfolding transition, as monitored by changes in the fluorescence intensity at 360 nm, shows a single transition. At low pH, the transition again appears to be a single transition. In the range of 3.5–6.0, the transition is biphasic, indicating the existence of a folding intermediate. The transitions have also been studied using circular dichroism and size exclusion chromatography. The data were fitted by a model in which the dimeric protein first unfolds to form structured monomers, followed by the unfolding of the monomers. From fits with this "folded monomers" model, the free energy change for the dimer ⇌ monomer dissociation becomes less positive as pH is decreased; the free energy change for the unfolding of the monomers is essentially independent of pH. An alternate model is one in which the dimer first undergoes a transition to a partially unfolded dimeric state, with this intermediate then denaturing to unfolded monomers. Both models give adequate fits to the data obtained at a single protein concentration. From a study of the concentration dependence of the urea-induced unfolding at pH 5, the "folded monomers" model is found to be more consistent with the data. Size exclusion chromatography data support the description of the intermediate state, which is the most populated state at low pH in the absence of urea, as being a relatively compact monomer. Circular dichroism studies show this intermediate to have a significant degree of secondary structure but to have a disorganized tertiary structure.

The *trp* aporepressor (*trpR*)[1] is a small, homodimeric protein (M_R = 12.5K per subunit) that has its two subunits intertwined (Joachimiak *et al.*, 1983; Schevitz *et al.*, 1985). Upon binding tryptophan ligands in its two binding sites, *trpR* undergoes a conformational change that enables its two helix–turn–helix motifs to interact strongly and specifically with operator regions of the *trp* operon (Zhang *et al.*, 1987). Due to its intertwined quaternary structure and because it is a prototypical regulatory protein of transcription, there has been interest in studying the thermodynamics and kinetics of unfolding of this protein.

Lane and Jardetzky (1987) studied the urea-induced unfolding of *trpR* at pH 7.6 by a combination of steady-state fluorescence, circular dichroism (CD), and ^{1}H NMR methods and reported that unfolding proceeds by formation of a folding intermediate. These researchers concluded that this intermediate is a dimeric state (see model 3 below). Using difference spectroscopy, steady-state fluorescence, and CD, Gittleman and Matthews (1990) also studied the thermodynamics of the urea-induced unfolding of *trpR* at pH 7.6. They found a monophasic[2] unfolding transition and concluded that there is not a significant population of an unfolding intermediate. Very recently Mann *et al.* (1993) have performed a comparative study of the urea-induced unfolding of wild-type *trpR* and two single tryptophan-containing mutants of this protein. They reported that an unfolding intermediate can be detected for the mutants, but not for the wild-type (again at pH 7.6). Finally, Fernando and Royer (1992b) have used time-resolved fluorescence methods to monitor the unfolding transitions and to characterize the initial and final states. These workers have measured the fluorescence spectrum and anisotropy of *trpR* as a function of protein concentration at neutral pH and have observed changes that are believed to reflect the dissociation (in the absence of denaturant) of the subunits at concentrations below 1×10^{-7} M (Fernando & Royer, 1992a).

Our laboratory has studied the thermodynamics of the binding of specific ligands to *trpR* (Hu & Eftink, 1993, 1994) and has found a pH dependence to ligand binding (Hu & Eftink, 1993; Hu, 1993). We initiated a study of the pH dependence of the urea-induced unfolding of *trpR* to see if it would provide insight about the pH dependence of ligand binding and to see if unequivocal evidence for an unfolding

† This research was supported by NSF Grant DMB 91-06377.

* To whom correspondence should be addressed.

® Abstract published in *Advance ACS Abstracts,* August 1, 1994.

[1] Abbreviations: D, native dimer of *trpR*; D′, partially unfolded dimer; N, folded monomer; U, unfolded monomer; ΔG°_{un}, standard free energy change for unfolding transition as a function of [denaturant]; $\Delta G^\circ_{0,un}$, standard free energy change for an unfolding transition in the absence of denaturant at reference condition; K_{un}, equilibrium constant for unfolding reaction; $K_{un,D\rightleftharpoons 2N}$, $K_{un,N\rightleftharpoons U}$, $K_{un,D\rightleftharpoons D'}$, and $K_{un,D'\rightleftharpoons 2U}$, equilibrium constants for transitions between the D ⇌ 2N, N ⇌ U, D ⇌ D′, and D′ ⇌ 2U states; *m*, index for urea-induced unfolding, $d\Delta G^\circ_{un}/d[\text{denaturant}]$; $[P]_o$, total concentration of *trpR* expressed as monomers; *trpR*, *trp* aporepressor from *Escherichia coli*; X_i, X_D, $X_{D'}$, X_N, X_U, mole fraction of states *i*, D, D′, N, and U.

[2] We define monophasic to be a transition between two states (spectroscopic signals), biphasic to be a process that involves a two-step transition between three states (signals), etc.

0006-2960/94/0433-10220$04.50/0

intermediate could be obtained at other pH.

MATERIALS AND METHODS

Materials

Apo *trpR* was isolated from an *Escherichia coli* cell line CY15071 that contains PJPR2 plasmid, which contains the *trpR* gene and an ampicillin-resistant gene. The isolation procedure was that of Joachimiak *et al.* (1983), with minor modifications. Details of the isolation procedure and materials used are given in Helton (1993). Following the phosphocellulose ion-exchange chromatography step, the protein was found to show a single peak on capillary electrophoresis (native conditions) and SDS–polyacrylamide gel electrophoresis. The protein was dialyzed against 0.1 M KCl, 0.01 M potassium phosphate, and 1.5 mM EDTA, pH 7, buffer and was stored at −70 °C. Protein concentration was determined spectrophotometrically using an extinction coefficient of 2.97×10^4 M^{-1} cm^{-1} for the dimer.

The unfolding studies were performed with solutions that contained approximately 1×10^{-6} M *trpR* dimer (except in cases where the protein concentration was varied) and with solutions that contained 0.01 M buffer salt and 0.1 mM EDTA. These concentrations of buffer and EDTA were chosen to be the same as that used by Gittelman and Matthews (1990). The buffers were sodium acetate, pH 2.5–5.5, sodium phosphate, pH 6–8, and sodium carbonate, pH 9–12. All solutions were prepared with distilled, deionized water. The stored, frozen protein samples were thawed and dialyzed against the desired buffer, passed through a Millipore filter, and then diluted with the buffer (or urea solution) for the spectroscopic studies. For studies at pH 4–5.5, it was found that the protein solutions are turbid. Since the isoelectric point of *trpR* is 5.9 (Joachimiak *et al.*, 1983), this turbidity most likely is due to aggregation of the protein. We have not attempted to characterize this aggregation phenomenon. Fernando and Royer (1992a, 1993) have observed some aggregation of *trpR* at neutral pH and have reported that the extent of aggregation decreases with increasing ionic strength. Our use of low ionic strength in the unfolding studies may exacerbate the aggregation, but we do not find noticeable turbidity for solutions at pH above 6 or below 3. For studies between pH 4 and pH 5.5, we have dialyzed the protein sample versus a pH ~7, 0.01 M sodium acetate buffer, before filtering and diluting the protein solution into a buffered solution having the desired pH. To further avoid problems of turbidity in the fluorescence studies (see below), we used 4- or 2-mm path cuvettes, and we monitored the emission at a wavelength that is far removed from the light scattering signals.

Urea solutions were used the same day that they were prepared. Ultrapure urea was obtained from United States Biochemical Corp. and was dissolved in the desired buffer to a concentration of 10 M. The pH of the urea solutions was adjusted, when necessary, to the desired value.

Methods

Steady-state fluorescence measurements were made with a Perkin-Elmer MPF 44A spectrophotofluorometer. Temperature was maintained at 25 °C with a thermojacketed cell holder. Measurements were made with an excitation wavelength of 295 nm, an emission wavelength of 360 nm, and 5-nm slits.

Unfolding experiments were performed by the method of Job. Two solutions were prepared, one containing the protein in buffer and the other containing the protein in an ~10 M urea solution (also buffered). Aliquots from one solution were added to the other (and vice versa) and fluorescence was measured. In the transition range, care was taken to allow sufficient time for equilibrium to be reached. Reversibility of the unfolding process at each pH was demonstrated by good agreement of the upward and downward titrations. The fluorescence versus [urea] data were analyzed in terms of either the three models presented in the next section.

The fluorescence data in Figures 2 and 3 have been made relative to the fluorescence of *trpR* in 8 M urea. That is, a solution of *trpR* in 8 M urea was subjected to a pH titration from pH 2.5 to pH 12, with fluorescence intensities being measured. A decrease in fluorescence with decreasing pH was observed; the pattern was gradual and did not suggest a simple proton ionization equilibrium. The fluorescence of any other protein solution was normalized to this pH dependence at 8 M urea.

Circular dichroism spectra were measured with an AVIV 62 DS instrument, which has been modified to simultaneously monitor steady-state fluorescence and which is equipped with a thermoelectric cell holder (Ramsay & Eftink, 1994). Some unfolding experiments were performed with this instrument, with simultaneous monitoring of fluorescence and far-UV CD signals. Urea was added via a computer-controlled dispenser, and the CD and fluorescence data as a function of [urea] were globally analyzed in terms of the models presented in the section below. A thorough description of the automatic titration system, controlling software, and data analysis procedures will be presented elsewhere.

Size exclusion chromatography (SEC) was performed using an ISCO 2350 HPLC pump, a TSK-2000 analytical column, a Sargent-Welch 550 single-beam UV–vis spectrophotometer and flow cell, and an HP 3394A integrating recorder. A flow rate of 1 mL/min was used. The temperature within the column was maintained at 20 °C using a homemade water jacket. The elution volume, V, of a sample was converted to a partition coefficient, K_D, by the relationship $K_D = (V_T - V)/(V_T - V_0)$, where V_T is the total volume of the column (determined as the elution volume of NaN_3) and V_0 is the void volume (determined by the elution of blue dextran). The elution of molecular weight standards (Bio-Rad, Inc.) was used to show that the characteristics of this column are similar to those used by Corbett and Roche (1984), thus enabling us to relate our K_D values to the hydrodynamic radii of the proteins studied by these researchers.

MODELS

The urea-induced changes in the steady-state fluorescence intensity of *trpR* were analyzed in terms of the following models. The fluorescence intensity, F, was used because such data (unlike emission λ_{max}) are directly related to the mole fraction of molecules in a given state via the following (Eftink, 1994):

$$F = \sum X_i F_i \tag{1}$$

where X_i is mole fraction and F_i is the intrinsic, relative fluorescence of state i. The values of X_i are calculated for the different models as described below. Also, in each case the equilibrium constants were assumed to depend on the concentration of urea according to the linear free energy relationship (Schellman, 1978; Pace, 1986, 1989):

$$\Delta G^\circ_{un} = \Delta G^\circ_{0,un} - m[\text{urea}] \tag{2}$$

where $\Delta G°_{un} = RT \ln K_{un}$ is the free energy change for unfolding and $\Delta G°_{0,un}$ is the free energy change in the absence of urea.

The intrinsic fluorecence of each state, F_i, was allowed to have an intrinsic dependence (i.e., a base-line slope) on the concentration of urea according to the following relationship:

$$F_i = F_{0,i} + s_i[\text{urea}] \tag{3}$$

where $F_{0,i}$ is the intensity of the state in the absence of urea and slope s_i is the dependence of F_i on urea concentration.

In the fits described below, the $\Delta G°_{0,un}$ and m for each transition and the $F_{0,i}$ and s_i are floated as fitting parameters. In the case of an intermediate state we made the assumption that its slope, s_i, was the average of the slope of the completely folded and unfolded states. The models were fitted using the nonlinear least-squares program, NONLIN (Johnson & Fraiser, 1985).

Two-State Model. This model assumes that the protein exists only as a native dimer, D, and unfolded monomers, U, as follows:

$$D \rightleftharpoons 2U \tag{4}$$

$$K_{un} = [U]^2/[D] \tag{5}$$

$$Q = 1 + K_{un}^{1/2}[D]^{-1/2}/2 \tag{6}$$

$$X_D = 1/Q \qquad X_U = K_{un}^{1/2}[D]^{-1/2}/2Q \tag{7}$$

where Q is the molar partition coefficient. The free concentration of the native dimer, [D], is related to the concentration of protein, expressed as the total concentration of subunits, $[P]_0$, as $[P]_0 = 2[D] + [U] = 2[D] + (K_{un}[D])^{1/2}$. The quadratic solution for the latter equation yields, with eq 5, the following:

$$X_U = \frac{(K_{un}^2 + 8K_{un}[P]_0)^{1/2} - K_{un}}{4[P]_0} \tag{8}$$

A nonlinear least-squares program was written that combines eqs 8 and 1–3 to fit this model to experimental data.

Three-State Model (Folded Monomers Model). This model assumes that there is a two-step (three-state) unfolding process, with the formation of a folded monomeric intermediate, N. By "folded" we mean that the intermediate can be further unfolded, in a cooperative manner, by the addition of urea. It is not known to what extent the intermediate's structure actually resembles the subunits of the native dimer.

$$D \rightleftharpoons 2N \rightleftharpoons 2U \tag{9}$$

The equilibrium constants for this model are defined as $K_{un,D\rightleftharpoons 2N} = [N]^2/[D]$ and $K_{un,N\rightleftharpoons U} = [U]/[N]$, where $K_{un,D\rightleftharpoons 2N}$ is a subunit dissociation process and $K_{un,N\rightleftharpoons U}$ is a unimolecular isomerization (unfolding). The expressions for the mole fraction of the D, N, and U states are

$$X_N = 1/Q; X_D = ([N]/K_{un,D\rightleftharpoons 2N})/Q; \quad X_U = 1 - X_D - X_N \tag{10}$$

where $Q = 1 + [N]/K_{un,D\rightleftharpoons 2N} + K_{un,N\rightleftharpoons U}$. From the expression for the conservation of mass ($[P]_o = 2[D] + [N] + [U] = 2[N]_2/K_{un,D\rightleftharpoons 2N} + [N] + K_{un,N\rightleftharpoons U}[N]$), the free concentration of folded monomer, [N], is

$$[N] = [-(K_{un,D\rightleftharpoons 2N} + K_{un,D\rightleftharpoons 2N}K_{un,N\rightleftharpoons U}) + \{(K_{un,D\rightleftharpoons 2N} + K_{un,D\rightleftharpoons 2N}K_{un,N\rightleftharpoons U})^2 + 8K_{un,D\rightleftharpoons 2N}[P]_0\}^{1/2}]/4 \tag{11}$$

By combining eqs 11, 10, and 1–3, a relationship is obtained to relate this model to experimental data.

Three-State Model (Partially Unfolded Dimer Model). This model also considers the existence of an intermediate in the unfolding process. The intermediate is a partially unfolded dimeric state, D′, which can then be further unfolded to unfolded monomers. The term "partially unfolded dimer" is taken to mean a state that cooperatively forms from the native dimer state; the term does not imply anything about the intermediate's structure.

$$D \rightleftharpoons D' \rightleftharpoons 2U \tag{12}$$

From the definition of isomerization equilibrium constant $K_{un,D\rightleftharpoons D'} = [D']/[D]$ and dissociation equilibrium constant $K_{un,D'\rightleftharpoons 2U} = [U]^2/[D']$, the following expressions for the mole fractions result:

$$X_U = 1/Q; \quad X_{D'} = ([U]/K_{un,D'\rightleftharpoons 2U})/Q; \quad X_D = 1 - X_U - X_D \tag{13}$$

where $Q = 1 + [U]/K_{un,D'\rightleftharpoons 2U} + [U]/(K_{un,D\rightleftharpoons D'}K_{un,D'\rightleftharpoons 2U})$. From the conservation of mass ($[P]_0 = 2[D] + 2[D'] + [U] = 2[U]^2/(K_{un,D\rightleftharpoons D'}K_{un,D'\rightleftharpoons 2U}) + 2[U]^2/K_{un,D'\rightleftharpoons 2U} + [U]$), the concentration of unfolded monomer is

$$[U] = [-1 + \{1 + 8[P]_0[1/(K_{un,D\rightleftharpoons D'}K_{un,D'\rightleftharpoons 2U}) + 1/K_{un,D'\rightleftharpoons 2U}]\}^{1/2}]/\{(4)[1/(K_{un,D\rightleftharpoons D'}K_{un,D'\rightleftharpoons 2U}) + 1/K_{un,D'\rightleftharpoons 2U}]\} \tag{14}$$

By combining eqs 14, 13, and 1–3, this model was fitted to experimental data via a nonlinear least-squares program.

RESULTS

Steady-State Fluorescence Spectra. In Figure 1 are shown emission spectra of *trpR* in the absence and presence of 9.94 M urea at pH 2.5 and 7 (spectra at pH 12 are not shown but are very similar to those at pH 7). At neutral and high pH, unfolding of the protein results in a large red shift (329 nm to 350 nm) and a small increase in the overall intensity of the emission from the two tryptophan residues, Trp19 and Trp119, in *trpR*. At pH 2.5, unfolding results in a red shift (339 nm to 351 nm) and a sizable decrease in emission intensity. In each case, there is a change in the intensity at 360 nm, and this wavelength was used to monitor changes upon the addition of urea. This wavelength was also chosen because it avoids Rayleigh and Raman scattering signals, which are significant in the pH range of 4–5, where the solutions are turbid due to aggregation of the protein.

Fluorescence Urea Titrations. Shown in Figure 2 are urea titrations of the fluorescence of *trpR* at neutral to high pH (pH 7–12). The patterns are monophasic and are very similar, showing an increase in fluorescence as urea is added. In each of these cases, the data can be adequately described by the two-state unfolding model in which the protein exists either as a folded dimer or as unfolded monomeric subunits. This model includes an intrinsic protein concentration dependence, since it is a dimer to monomer transition. Gittleman and Matthews (1990) have demonstrated that the urea-induced unfolding of *trpR* shows this dependence on protein concentration. There is no evidence for an unfolding intermediate in this pH range. The solid lines in Figure 2 are fits of the

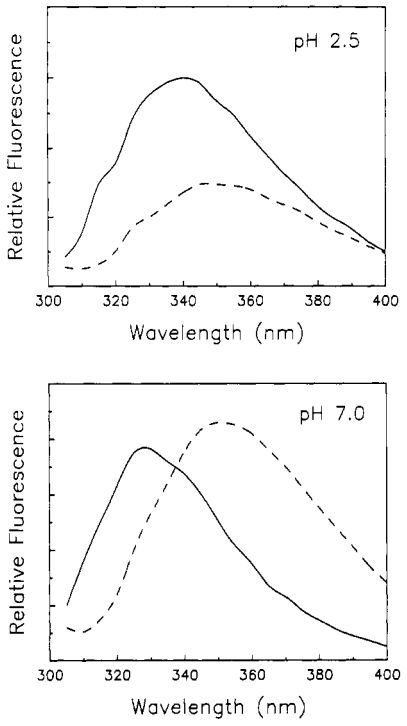

FIGURE 1: Fluorescence emission spectra of *trpR* in the absence (solid lines) and presence (dashed lines) of 9.96 M urea at pH 2.5 (top panel) and pH 7.0 (bottom panel). Conditions: excitation wavelength of 295 nm, 5-nm slits, 25 °C.

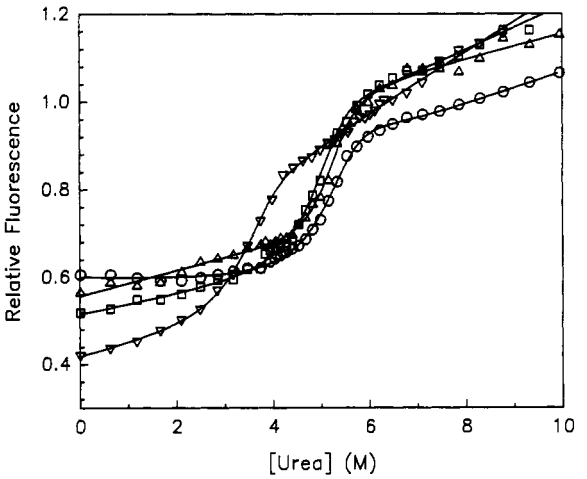

FIGURE 2: Dependence of the fluorescence intensity (at 360 nm) of *trpR* on [urea] at pH 7 (○), pH 9 (△), pH 11 (□), and pH 12 (▽). The solid lines are fits of eqs 1 and 2 and the two-state model (eqs 3–7) to the data.

two-state model with $\Delta G°_{0,un}$ values given in Figure 4A. For example, at pH 7 a fit is obtained with $\Delta G°_{0,un} = 21.0 \pm 3.0$ kcal/mol and $m = 2.58 \pm 0.6$ kcal/mol (and with intensities of the native and unfolded state of 0.59 and 0.74, respectively, and with slopes of the relative fluorescence of the native and unfolded states of 0.006 and 0.03 M^{-1}, respectively). For data between pH 7and pH 11, the $\Delta G°_{0,un}$ are in the range of 21–24 kcal/mol, with a drop at pH 12. The urea m value was approximately the same over this pH range, with an average value of 2.7 ± 0.4 kcal/mol.

Shown in Figure 3 are urea titrations of the fluorescence of *trpR* at neutral to low pH (pH 7–3). Whereas at neutral pH the transition is monophasic, at pH between 3.5 and 5.0, the transition is clearly biphasic and cannot be adequately described by the two-state unfolding model. For example, at pH 5, as urea is added, there is an increase in fluorescence

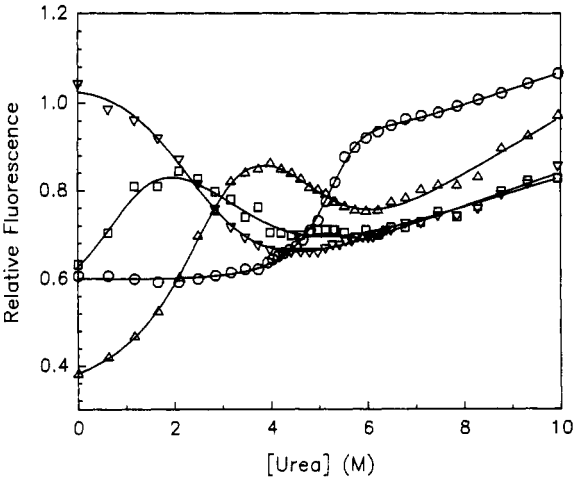

FIGURE 3: Dependence of the fluorescence intensity (at 360 nm) of *trpR* on [urea] at pH 7 (○), pH 5 (△), pH 4 (□), and pH 3 (▽). The lines are fits of eqs 1 and 2 and the *folded monomers* model (eqs 8–10). A fit of the *partially unfolded dimer* model is a nearly indistinguishable fit.

between 0 and 4 M urea, reaching a maximum at [urea] = 4 M, and then there is a decrease in intensity as the urea concentration is further increased to 6 M. The position of the intensity maximum shifts to lower [urea] as pH is decreased. At the lowest pH investigated, pH 2.5 and 3, the transition again appears to be monophasic, with the intensity decreasing as urea is added.

The data between pH 3.5–6.0 cannot be adequately described by a two-state model. Instead, a three-state (*folded monomers*) model with an unfolding intermediate is required to achieve an adequate fit (see the Discussion for the description of these fits, which are shown by the solid lines in Figure 3). The $\Delta G°$ values for this *folded monomers* model are plotted in Figure 4A. The fits call for the fluorescence intensity of the folded monomer intermediate to be about twice as large as the intensity of the native dimer and to also be larger than the intensity of the unfolded monomer.

Urea unfolding at pH 5 was studied as a function of protein concentration, in order to discriminate between the above three-state unfolding models (i.e., the *folded monomers* model and the *partially unfolded dimer* model). These data are shown in Figure 5. The protein concentration range was from 0.13 × 10^{-5} to 1.3 × 10^{-5} M (expressed as total concentration of dimer). As can be seen, the "hump" becomes more pronounced and moves to lower urea concentration as the protein concentration is decreased. The solid lines through these data are a global fit of the three data sets to the *folded monomers* model, as will be described in the Discussion.

Circular Dichroism Data. Figure 6 shows the aromatic CD and far-UV CD spectra of *trpR* at pH 7 and 2.6 (absence of urea). At pH 7 the far-UV CD spectrum is similar to that previously reported at pH 7.6 (Mann & Matthews, 1993). Analysis via the secondary structure algorithm of Yang *et al.* (1986) gives a value of 51% α-helix for the protein at neutral pH. At pH 2.6 the far-UV CD spectrum is slightly less pronounced, indicating retention of a large degree of secondary structure. The aromatic CD region shows fine structure at neutral pH, but no structure for the low-pH form.

Using our multidimensional spectrophotometer (Ramsay & Eftink, 1994), we have simultaneously monitored changes in CD and fluorescence as a function of [urea]. Shown in Figure 7 are such data (with CD at both 220 and 230 nm) obtained at three pHs. The combined data sets were globally analyzed in terms of the above models (see the Discussion).

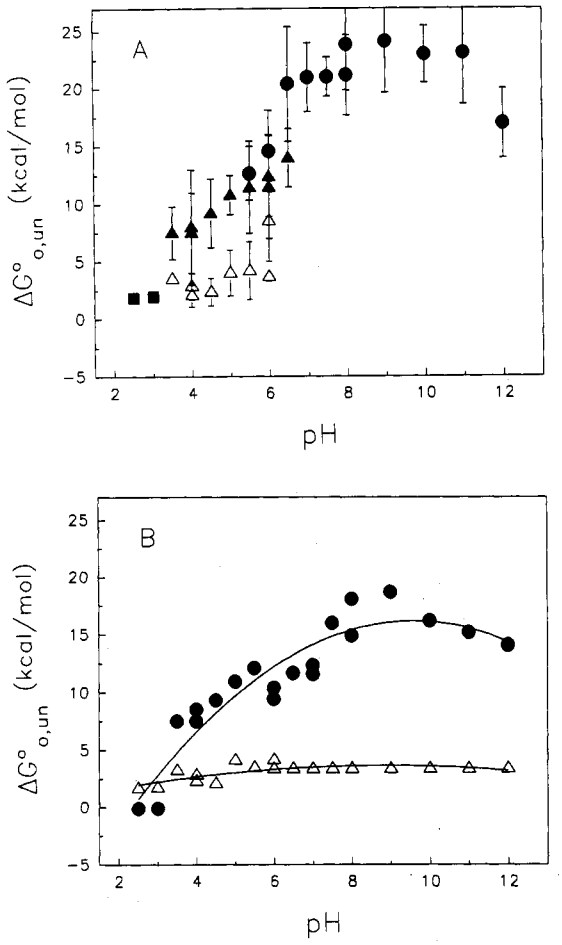

FIGURE 4: (A) Free energy changes for the urea-induced unfolding of *trpR* as a function of pH. Closed circles (●) between pH 5.5 and 12 are fits to a two-state D ⇌ 2U unfolding model. Closed squares (■) between pH 2.5 and 3 are for fits to a two-state N ⇌ U model. Between pH 3.5 and 6 the data were fitted to a three-state D ⇌ 2 N ⇌ 2U model with the closed triangles (▲) being the $\Delta G^\circ_{0,D\rightleftharpoons 2N}$ for the dimer dissociation step and open triangles (△) being the $\Delta G^\circ_{0,N\rightleftharpoons U}$ for the unfolding of the folded monomer. (B) Analysis according to the three-state *folded monomers* model over the entire pH range; shown are the resulting $\Delta G^\circ_{0,D\rightleftharpoons 2N}$ (●) and $\Delta G^\circ_{0,N\rightleftharpoons U}$ (○). In this partially constrained fit, the value of $\Delta G^\circ_{0,D\rightleftharpoons 2N}$ was fixed at −0.1 kcal/mol at pH 2.5–3 and the value of $\Delta G^\circ_{0,N\rightleftharpoons U}$ was fixed at 3.4 kcal/mol (and the corresponding m was fixed at 0.8 kcal/mol) at pH 6.5 and above. The solid lines are not theoretical curves but trace the trends.

Size Exclusion Chromatography. The unfolding of the protein was also studied by SEC at pH 5.0 and 2.5. Shown in Figure 8 is a plot of the partition coefficient, K_D, as a function of [urea]. The K_D value is 0.6 at pH 5 in the absence of urea and decreases as urea is added, indicating that the hydrodynamic radius of the protein increases as it unfolds. The transition appears to be biphasic at pH 5.0, with there being a slight increase in K_D between 0 and 3 M urea and a larger decrease in K_D between 3 and 6 M urea.

At pH 2.5 the K_D is 0.68 in the absence of urea and there is a monophasic decrease in K_D as [urea] is increased to a limiting value of 0.36, indicating an increase in hydrodynamic radius as the protein is perturbed. The line through the low-pH data is a fit of a two-state unfolding model (N ⇌ U, where N is a monomeric folded state) with $\Delta G^\circ_{0,un}$ = 2.1 kcal/mol and m = 0.75 kcal/mol. (The SEC studies were done in a buffer of 0.1 M Na_2SO_4, 0.01 M sodium acetate, and 0.1 mM EDTA. A higher ionic strength, in comparison with that in the spectroscopic studies, is needed to avoid nonspecific absorption of the protein to the column matrix.)

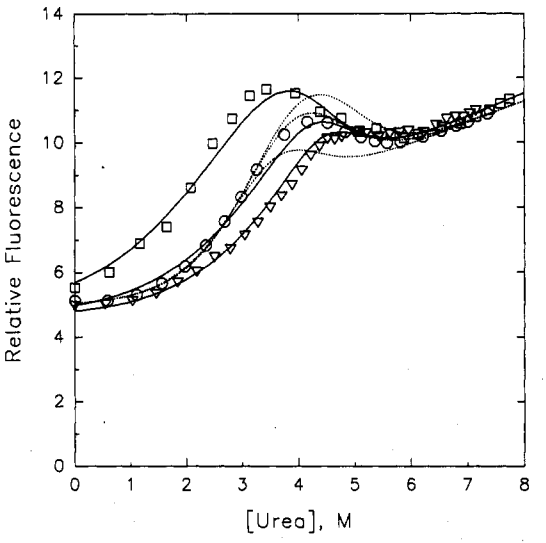

FIGURE 5: Dependence of the urea-induced unfolding of *trpR* on protein concentration: 1.3 × 10^{-5} M (▽); 0.63 × 10^{-5} M (○); and 0.13 × 10^{-5} M (□). The solid lines are a simultaneous fit of the three data sets to the *folded monomers* model with $\Delta G^\circ_{0,D\rightleftharpoons 2N}$ = 9.7 kcal/mol, $m_{D\rightleftharpoons 2N}$ = 0.8 kcal/(mol·M), $\Delta G^\circ_{0,N\rightleftharpoons U}$ = 5.0 kcal/mol, and $m_{N\rightleftharpoons U}$ = 1.1 kcal/(mol·M). The dashed lines are an attempted fit of the *partially unfolded dimer* model to the data as described in the text; the upper dashed line is for the higher protein concentration, and the lower dashed line is for the lower protein concentration. The latter model adequately describes the intermediate protein concentration data (as illustrated by the middle dashed line), with $\Delta G^\circ_{0,D\rightleftharpoons D'}$ = 2.82 kcal/mol, $m_{D\rightleftharpoons D'}$ = 0.78 kcal/(mol·M), $\Delta G^\circ_{0,D'\rightleftharpoons 2U}$ = 12.0 kcal/mol, and $m_{D'\rightleftharpoons 2U}$ = 1.26 kcal/(mol·M), but fails in the global analysis of the three concentrations.

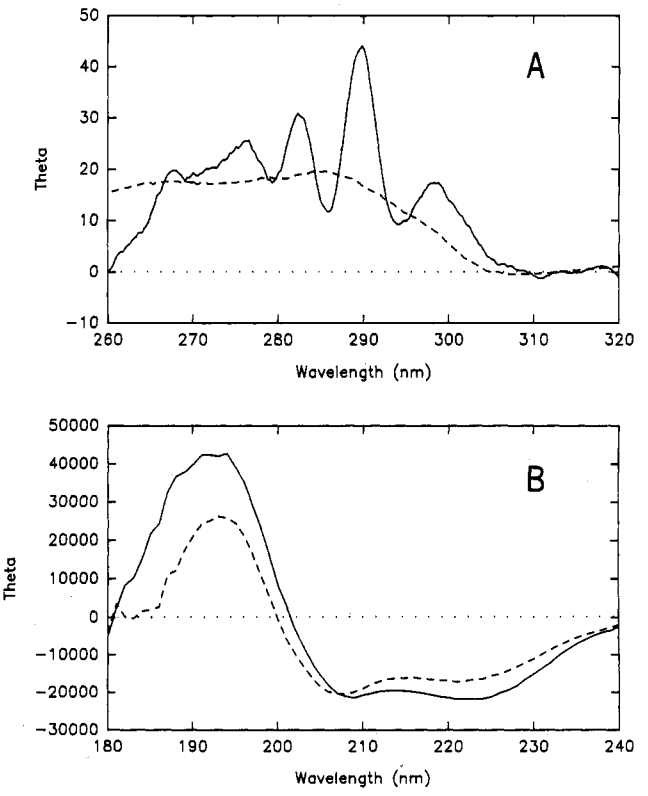

FIGURE 6: (A) Aromatic circular dichroism spectra for *trpR* at pH 7.5 (—) and pH 2.6 (- - -). (B) Far-UV circular dichroism spectra for *trpR* at pH 7.5 (—) and pH 2.6 (- - -). Spectra taken at 25 °C.

DISCUSSION

We will first discuss the evidence for the existence of an equilibrium intermediate in the unfolding of *trpR* at low pH. Then we will discuss thermodynamic data and a model for the

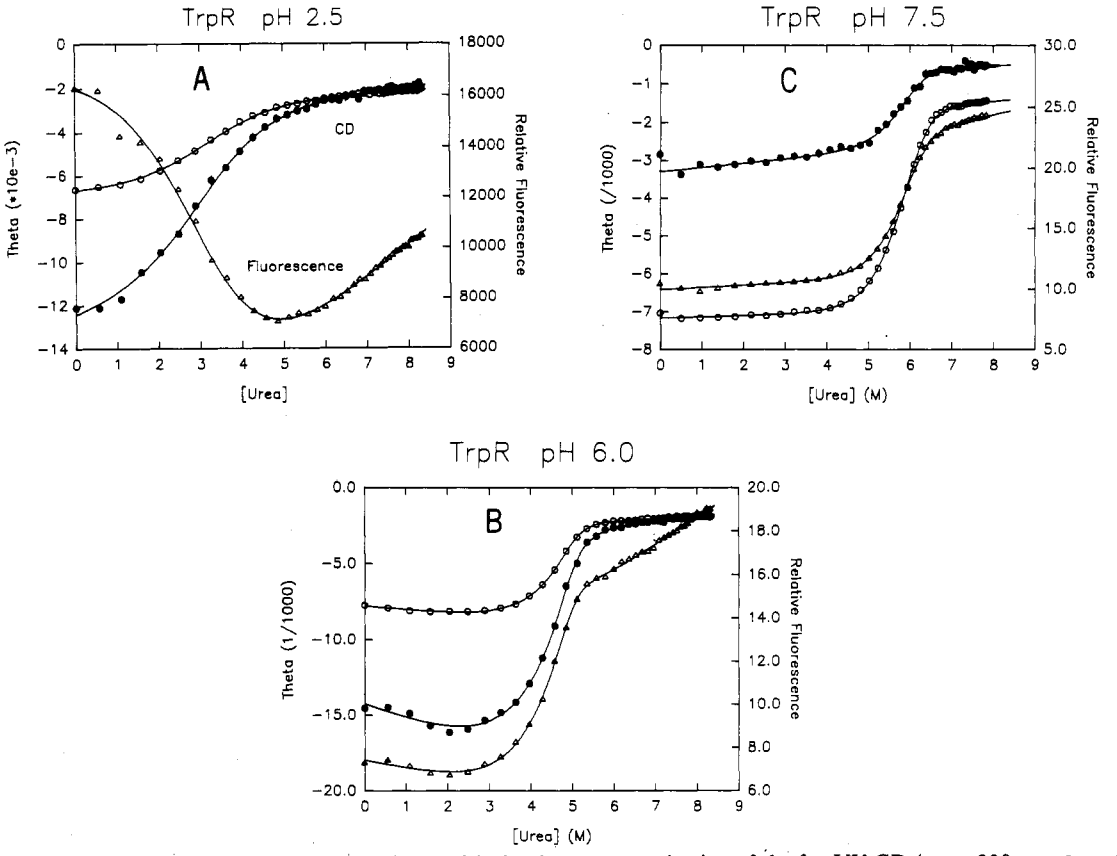

FIGURE 7: Urea unfolding of *trpR* at pH 2.5, 6, and 7.5, with simultaneous monitoring of the far-UV CD (●, at 220 nm; ○, at 230 nm) and steady-state fluorescence (△, emission at 360 nm, excitation at 295 nm). For the pH 2.5 and 7.5 data, the solid lines show a global fit to the two-state unfolding model. For the pH 6 data, the solid lines show a global fit to the *folded monomers* model, which is required for an adequate, global fit of the three data sets. The global fitting parameters are as follows: at pH 7.5, $\Delta G^\circ_{0,un}$ = 26.6 ± 1.0 kcal/mol, m = 2.38 ± 0.2 kcal/(mol·M); at pH 2.5, $\Delta G^\circ_{0,un}$ = 2.2 ± 0.3 kcal/mol, m = 0.70 ± 0.05 kcal/(mol·M); at pH 6.0, $\Delta G^\circ_{0,D\rightleftharpoons 2N}$ = 13.0 ± 1.0 kcal/mol, $m_{D\rightleftharpoons 2N}$ = 1.32 ± 0.3 kcal/(mol·M), $\Delta G^\circ_{0,N\rightleftharpoons U}$ = 8.0 ± 2.0 kcal/mol, and $m_{N\rightleftharpoons U}$ = 1.6 ± 0.4 kcal/(mol·M).

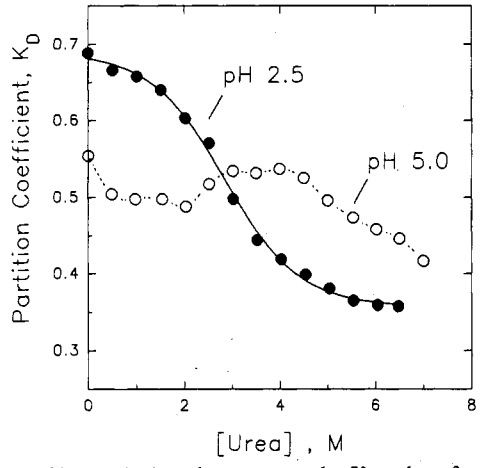

FIGURE 8: Size exclusion chromatography K_D values for *trpR* as a function of [urea] at pH 5 (open circles) and at pH 3 (closed circles) at 25 °C. The line through the pH 2.5 data is a fit to a two-state urea-induced unfolding model with a free energy change for unfolding (in the absence of urea) of 2.1 ± 0.2 kcal/mol, a urea "m" value of 0.75 ± 0.06 kcal/mol, a K_D for the folded state of 0.689 ± 0.007 and a K_D for the unfolded form of 0.357 ± 0.005. The dashed line through the pH 5 data is not a theoretical fit.

subunit dissociation and unfolding transitions. Finally, we will interpret spectroscopic and chromatographic data regarding the structure of the folding intermediate.

Evidence for a Folding Intermediate. The urea-induced changes in the fluorescence of *trpR* are monophasic and consistent with a two-state unfolding transition at neutral and higher pH, as previously reported by Gittleman and Matthews (1990). As the pH is lowered, however, the data in Figure 3 show a biphasic transition. In the pH range of 3.5–6, the fluorescence at 360 nm increases, reaches a maximum, and then decreases and reaches a final, positively sloping post-transition baseline. This multiphasic pattern indicates that there must be an unfolding intermediate in this pH range. The position of the hump moves to lower [urea] as pH is lowered. At pH 3.0 the hump has disappeared. At and below this pH the fluorescence change is again monophasic; the fluorescence decreases with increasing [urea] and reaches a final, positively sloping base line. The position of the hump (at pH 5) is also found to depend on protein concentration, as illustrated in Figure 5.

Additional evidence for the existence of a folding intermediate at pH 3.5–6 comes from simultaneous observation of urea-induced changes in the far-UV CD and fluorescence of *trpR*. As shown in Figure 7, CD and fluorescence signal changes occur in concert at pH 7.5 and 2.5, consistent with the transitions being essentially two-state at these pH values. At pH 6, however, the CD and fluorescence changes do not show identical transitions. Although it is difficult to see in Figure 7B, the midpoint of the CD transitions occurs at a higher [urea] than does the fluorescence transition. The fit shown through the three data sets in Figure 7B is to the *folded monomers* model, as discussed below.

The data in Figure 3 at pH 3.5–6, the protein concentration dependence data in Figure 5, and the simulataneously determined fluorescence and CD data in Figure 7B were fitted to the *folded monomers* model using eqs 1–3, 10, and 11 and a nonlinear least-squares program. The fits to the pH 3.5–6 data (solid lines in Figure 3) result in $\Delta G^\circ_{0,D\rightleftharpoons 2N}$ for the D $\rightleftharpoons$ 2N transition and the $\Delta G^\circ_{0,N\rightleftharpoons U}$ for the N $\rightleftharpoons$ U transition;

these free energy changes are plotted in Figure 4A. Likewise, the data for the protein concentration dependence at pH 5 in Figure 5 were globally fitted with this model with values of $\Delta G°_{0,D\rightleftharpoons 2N}$ = 9.7 kcal/mol and $\Delta G°_{0,N\rightleftharpoons U}$ = 5.0 kcal/mol. A reasonably good global fit is obtained for the three protein concentrations, as shown by the solid lines in Figure 5. We also attempted to fit the *partially unfolded dimer* model to these data. However, this model predicts an entirely different trend with increasing protein concentration. The dashed lines in Figure 5 show a pattern predicted by this model for increasing concentrations of protein. (It should be noted that the individual data sets at a single protein concentration can be adequately fitted by the *partially unfolded dimer* model, but the data in Figure 5 clearly enable us to eliminate this as an acceptable model for the unfolding process.) Finally, the simultaneously determined CD and fluorescence data at pH 6 in Figure 7B were globally fitted with the *folded monomers* model with $\Delta G°_{0,D\rightleftharpoons 2N}$ = 13.0 ± 1.0 kcal/mol and $\Delta G°_{0,N\rightleftharpoons U}$ = 8.0 ± 2.0 kcal/mol, as is shown by the solid lines. Thus, the various types of data, in the pH 3.5–6 range, are adequately described by a model in which there is a folded intermediate in the urea-induced transition.

pH Dependence of the Thermodynamics. The free energy change for the unfolding of *trpR* as a function of pH is shown in Figure 4A. The figure is divided into three regions. Above pH 6, the unfolding is described as a D ⇌ 2U two-state transition (solid circles), with the $\Delta G°_{0,un}$ reaching a maximum of nearly 24 kcal/mol over the pH range of 7–11 and then dropping slightly at pH 12.

The second region is between pH 2.5 and pH 3, where the transition is also two-state, and, based on the SEC data (and consistency with the model below), the transition is from a folded monomer, N, to an unfolded U. The $\Delta G°_{0,un}$ for the N ⇌ U transition is approximately 2 kcal/mol at this pH range (solid squares in Figure 4A); this value was determined by the spectroscopic studies in Figures 3 and 7A and the SEC data in Figure 8. The *m* value for the N ⇌ U transition is approximately 0.8 kcal/mol, as compared to a value of ~2.8 kcal/mol for the D ⇌ 2U transition.

The third region is between pH 3.5 and pH 6, where the unfolding can be described by a D ⇌ 2N ⇌ 2U "folded monomers" model. Shown in Figure 4A by the solid and open triangles are, respectively, the $\Delta G°_0$ for the D ⇌ 2N and N ⇌ U transitions. The free energy changes fall into a pattern that connects the two extreme pH regions. The fitted $\Delta G°_{0,N\rightleftharpoons U}$ values for the N ⇌ U transition are similar in magnitude to the $\Delta G°_{0,un}$ values for unfolding the low-pH state; the fitted $\Delta G°_{0,D\rightleftharpoons 2N}$ for the D ⇌ 2N transition shows an increase with increasing pH and approaches the $\Delta G°_{0,un}$ for the two-state D ⇌ 2U transition at neutral and high pH. (Actually, the value of $\Delta G°_{0,D\rightleftharpoons 2U}$ should be approximately equal to the sum of $\Delta G°_{0,D\rightleftharpoons 2N} + 2\Delta G°_{0,N\rightleftharpoons U}$.) Fitting for the separate $\Delta G°_0$ values for the D ⇌ 2N and N ⇌ U steps is difficult, due to the large number of fitting parameters (including the fluorescence intensities for each state and the base-line slopes, as well as the free energy and *m* values). Nevertheless, the pattern in Figure 4A indicates that the $\Delta G°_{0,D\rightleftharpoons 2N}$ for the D ⇌ 2N transition is much more dependent on pH than is the $\Delta G°_{0,N\rightleftharpoons U}$ for the N ⇌ U transition, with the latter free energy change being larger at pH 3 and below. Consequently, the N state becomes the most populated form of the protein in the absence of urea at low pH, thus making the N ⇌ U transition the dominant unfolding process. At neutral pH and above, $\Delta G°_{0,D\rightleftharpoons 2N}$ for dimer dissociation is so much larger in magnitude than the $\Delta G°_{0,N\rightleftharpoons U}$ for N ⇌ U unfolding that the overall urea unfolding process is indistinguishable from a two-state process (i.e., the dissociation step is energetically difficult and requires a high [urea]; once formed, the N state easily unfolds and never has a significant population).

Because the *folded monomers* model seems to describe the data between pH 3.5 and 6, we have analyzed the data at other pH according to this model. At pH above 6 this was done by fixing the value of $\Delta G°_{0,N\rightleftharpoons U}$ to be 3.4 kcal/mol and *m* to be 0.8 kcal/mol (which are average values for $\Delta G°_{0,N\rightleftharpoons U}$ and *m* for the pH range of 3.5–6). At pH 2.5–3 this was done by fixing $\Delta G°_{0,D\rightleftharpoons 2N}$ to be –0.1 kcal/mol and *m* to be zero, values which describe (along with the protein concentration) the dimer to be almost fully dissociated in the absence of urea. At pH 3.5–6 the fits were not constrained. As is shown in Figure 4B, this *folded monomers* model can describe the data over the entire pH range. We note that the three-state *folded monomers* model is a minimal model that describes the data; a more complicated model may also apply.

The ability to identify an equilibrium folding intermediate is due to the fact that $\Delta G°_{0,D\rightleftharpoons 2N}$ is attenuated by lowering pH to a much greater extent than is $\Delta G°_{0,N\rightleftharpoons U}$. It is only by studying the unfolding over a broad pH range that the existence of a folding intermediate is made evident. At neutral pH the dissociation of the subunits is an energetically difficult process and causes the overall unfolding process to be very cooperative. From inspection of the crystal structure of *trpR* dimer, it is obvious why the subunit association is so strong. The two subunits are intertwined. Apparently, the protonation of some groups at the intersubunit interface causes a reduction in the subunit association free energy. In fact, from the intertwined structure of *trpR* dimer, it is difficult to imagine that the monomer would have any stability as a folded state. Our analysis indicates that the folded monomer has a stability of ~3.4 kcal/mol at neutral pH (with a slightly lower stability of ~2 kcal/mol at acidic pH).

To illustrate the features of the *folded monomers model* and the thermodynamic parameters in Figure 4B, we have constructed the 3D plots of mole fraction of D and N states versus pH and [urea] in Figure 9A,B. Also shown in Figure 9C is a "phase diagram" for the transitions in the protein. The ordinate of this plot is the urea concentration corresponding to the $\Delta G°$ = 0 point of either the D ⇌ 2N or N ⇌ U transitions. The dominant species in each of the phase regions is indicated. This simulation was for a total protein subunit concentration of 5×10^{-6} M (approximately the concentration used in most of our studies). Since the D ⇌ 2N transition is concentration dependent, the position of this phase curve will shift to the right with decreasing protein concentration, whereas the N ⇌ U phase curve will not depend on concentration. We also show, by the dashed lines in Figure 9C, the effect of varying protein concentration from 5×10^{-5} to 5×10^{-7} M [the latter being the approximate cellular concentration of the protein (Gunsalus *et al.*, 1986)]. We reiterate that the simulations in Figure 9 are based on our conclusion that the *folded monomers model* is the more consistent model and on our assumption that the value of $\Delta G°_{0,N\rightleftharpoons U}$ is invariant above pH 6. Also, the diagrams in Figure 9 do not include the association of the protein to tetrameric and/or more highly aggregated forms that occurs at higher protein (Fernando & Royer, 1992a).

Relationship to Other Research. The kinetics and thermodynamics of the unfolding of oligomeric proteins have been extensively studied (Jaenicke, 1991). Homodimeric proteins provide the simplest systems. The unfolding of such dimeric

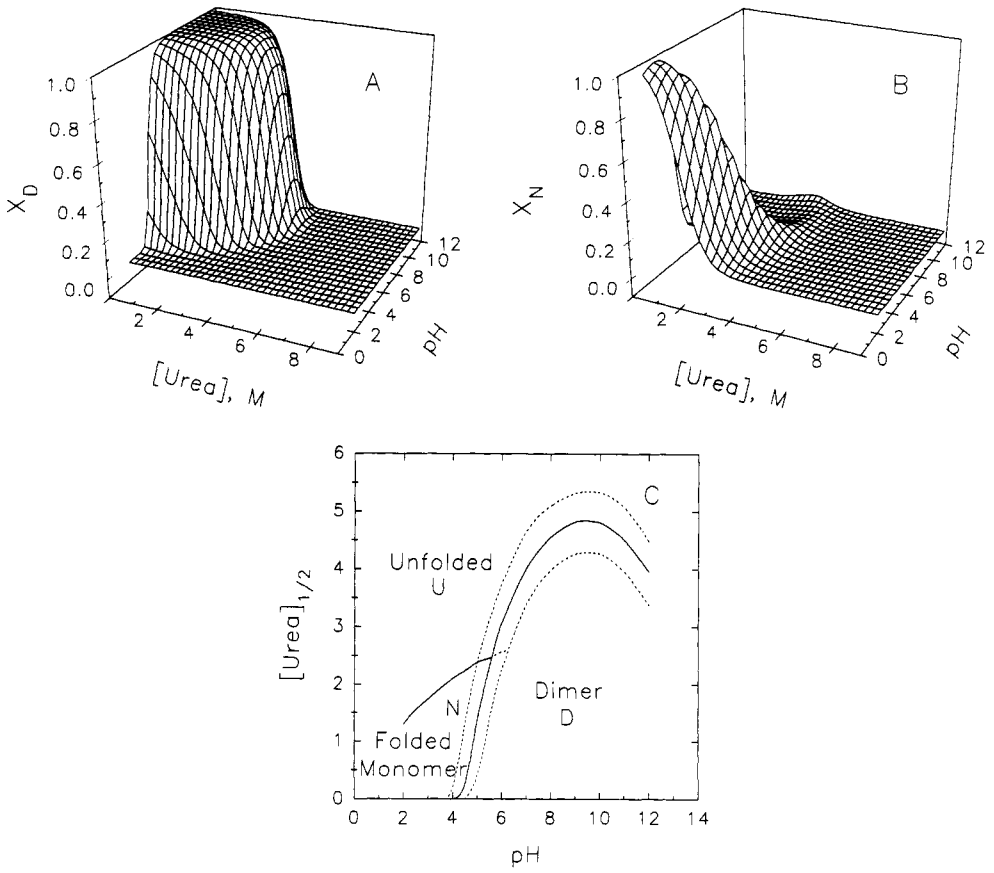

FIGURE 9: (A and B) Plots of the mole fraction of the native dimeric, D, and folded monomeric, N, states as a function of pH and [urea]. These plots were simulated using parameters from the polynomial fit of the free energy values in Figure 4B and the assumption that the *m* values were 1.3 kcal/(mol·M) for both the D ⇌ 2N and N ⇌ U transitions over the entire range. This latter assumption is made to simplify the simulation. A similar plot for the mole fraction of the U state is not shown. (C) "Phase diagram" for the urea- and pH-induced transitions of *trpR*. The dominant species in each phase region is labeled. The solid line corresponds to $\Delta G^\circ = 0$ combinations of pH and [urea] for the respective transitions. The simulation is for a concentration of protein subunits of 5×10^{-6} M. The dashed lines to the left and right are for simulations for 5×10^{-5} and 5×10^{-7} M, respectively, showing that the D ⇌ 2N transition will be concentration dependent.

proteins is frequently observed to be a two-state, D ⇌ 2U process; this has been found for Arc repressor (Bowie & Sauer, 1989; Silva *et al.*, 1992), λ Cro protein (Pakula & Sauer, 1989), the proteases from human immunodeficiency virus type 1 and simian immunodeficiency virus (Grant *et al.*, 1992), phosphoglucose isomerase (Blackburn & Noltmann, 1981), and *trpR* at neutral pH [Gittleman & Matthews (1990) and the data above], to name a few. A monomeric intermediate state, having a significant population, has been found for the guanidine-induced unfolding of dimeric aspartate aminotransferase (Herold & Kirschner, 1990). Several studies of the kinetics of unfolding/folding have identified transient intermediate states, but the most frequent observation is that the equilibrium population of such intermediates is small so that the unfolding transition appears to be two-state. The subunit–subunit interactions are so strong that, once a high enough denaturant concentration is reached to dissociate the subunits, the monomeric states are not sufficiently stable to remain folded. The work here shows that this is true at pH above ~6.5, but that the subunit–subunit interaction weakens at lower pH, allowing the monomeric state to be increasingly populated as pH is lowered.

Our results at neutral pH support the finding of Gittleman and Matthews (1990) that the urea-induced unfolding is essentially two-state in this pH region. Our data do not support the interpretation of Lane and Jardetzky (1987) that unfolding forms a partially unfolded dimeric state. The observation by Tasayco and Carey (1992) of a proteolytic dimeric fragment of *trpR* suggests that a partially unfolded dimeric folding intermediate may have significant stability. Of course, parallel unfolding paths may exist, and, as noted earlier, the D ⇌ 2N ⇌ 2U mechanism is only a minimal mechanism. However, this mechanism does fit a large amount of data as a function of pH and protein concentration and is consistent with the independent studies mentioned below.

Our $\Delta G^\circ_{0,D\rightleftharpoons 2N}$ and $\Delta G^\circ_{0,N\rightleftharpoons U}$ values can be compared to estimates of these values from previous work. In studies of the fluorescence of *trpR* as a function of concentration, Fernando and Royer (1992b) presented evidence that the K_D for the dissociation of the dimer is approximately 1×10^{-9} M at neutral pH. This K_D value leads to an estimate of $\Delta G^\circ_{0,D\rightleftharpoons 2N}$ = 13–14 kcal/mol (i.e., if it is assumed that the dimers dissociate into folded monomers, rather than completely unfolded monomers), which compares with our estimate of 14–15 kcal/mol for the $\Delta G^\circ_{0,D\rightleftharpoons 2N}$ step in Figure 4B at neutral pH. Combining Fernando and Royer's value of $\Delta G^\circ_{0,D\rightleftharpoons 2N}$ with the total free energy change for the urea-induced unfolding of the dimer at neutral pH leads to an independent estimate of 4.5 kcal/mol for the N ⇌ U transition, which compares with our analysis of 3.4 kcal/mol for the unfolding of the monomeric intermediate. Stopped-flow CD and ANS binding studies at pH 7.6 by Mann and Matthews (1993) have provided evidence for a transient, monomeric folding intermediate having a significant amount of secondary structure and hydrophobic surface. This intermediate was formed within the 4–5 ms mixing time, and the CD signal associated with this burst phase is very similar to that which we find (see Figure 6B) for the low-pH folded monomeric

state. From study of the urea concentration dependence of the burst CD amplitudes, Mann and Matthews determined that this transient intermediate has a free energy of stability of about 3.3 kcal/mol (and an m of ~0.9 kcal/(mol·M)), a value which is similar to the $\Delta G°_{0,N\rightleftharpoons U}$ (and m) that we have found for the stability of the monomeric intermediate from our equilibrium unfolding data.

Characterization of the Low-pH Folded State. Spectroscopic and chromatographic data reveal insight about the structure of the low-pH folded state of *trpR*. The fluorescence spectrum of this state (see Figure 1B) shows it to have a λ_{max} of 339 nm, which is red shifted to 351 nm upon urea unfolding. This indicates that the tryptophan residues are not fully exposed or solvent relaxed in the folded low-pH state. The CD spectra in Figure 6 show that a significant degree of α-helix still exists at pH 2.5 but that the chirality of the environment of the tryptophan residues has been lost. Together, the CD data suggest that the low-pH form retains secondary structure but does not have a definite tertiary structure. The SEC data in Figure 8 show the low-pH folded state to have a K_D of 0.68, as compared to a K_D of 0.55 for the native dimer at neutral pH and a K_D of 0.35–0.4 for the urea unfolded state at each pH. Using the set of K_D standards in Corbett and Roche (1989), we estimate hydrodynamic radii of 25–27, 34–36, and 43–45 Å for the low-pH state, the native dimer at neutral pH, and the urea unfolded forms. The fact that the radius of the low-pH state is smaller than that of the native dimer supports the notion that the low-pH state is a monomer and has a relatively compact average structure. Finally, the urea m value for the unfolding of the folded monomer (~0.8 kcal/mol) is lower than the m value for the D $\rightleftharpoons$ 2U unfolding transition (~2.8 kcal/mol). Since the magnitude of an m value can be related to the extent of change in the solvent exposure of apolar side chains upon unfolding (Pace *et al.*, 1989), the lower value of m for the N state indicates that the apolar side chains of this state are more solvent accessible than are the side chains of the native dimer (assuming that both form a similar U state having fully exposed side chains). Collectively, these results characterize the N state, which is the dominant state at low pH and which is a folding intermediate at pH 3.5–6, as being a relatively compact, monomeric, globular state, with a significant degree of α-helical secondary structure, with more exposed and disordered tryptophan residues, and with more overall accessibility of its apolar amino acid side chains, as compared to the native dimer. Such attributes have been referred to as a "molten globule" (Kawajima, 1989; Kim & Baldwin, 1990; Ptitsyn, 1987).

ACKNOWLEDGMENT

We thank Dr. Kathleen Matthews, Rice University, for providing us with the overproducing strain of bacteria. We thank Dr. Dana Hu and Cing-Yuen Wong for help in growing the bacteria and isolating the protein.

REFERENCES

Blackburn, M., & Noltmann, E. A. (1981) *Arch. Biochem. Biophys. 212*, 162–169.
Bowie, J. U., & Sauer, R. T. (1989) *Biochemistry 28*, 7139–7143.
Chou, W.-Y., Bieber, C., & Matthews, K. S. (1989) *J. Biol. Chem. 264*, 18309–18313.
Corbett, R. J. T., & Roche, R. S. (1984) *Biochemistry 23*, 1888–1894.
Eftink, M. R. (1994) *Biophys. J. 66*, 482–501.
Fernando, T., & Royer, C. A. (1992a) *Biochemistry 31*, 3429–3441.
Fernando, T., & Royer, C. A. (1992b) *Biochemistry 31*, 6683–6691.
Gittleman, M. S., & Matthews, C. R. (1990) *Biochemistry 29*, 7011–7020.
Grant, S. K., Deckman, I. C., Culp, J. S., Minnich, M. D., Brooks, I. S., Hensley, P., Debouck, C., & Meek, T. D. (1992) *Biochemistry 31*, 9491–9501.
Helton, K. J. (1993) Masters Thesis, University of Mississippi.
Herold, M., & Kirschner, K. (1990) *Biochemistry 29*, 1907–1913.
Hu, D. (1993) Ph.D. Dissertation, University of Mississippi.
Hu, D., & Eftink, M. R. (1993) *Arch. Biochem. Biophys. 305*, 588–594.
Hu, D., & Eftink, M. R. (1994) *Biophys. Chem. 49*, 233–239.
Jaenicke, R. (1991) *Biochemistry 30*, 3147–3161.
Joachimiak, A., Kelley, R. L., Gunsalus, R. P., Yanofsky, C., & Sigler, P. B. (1983) *Proc. Natl. Acad. Sci. U.S.A. 80*, 668–672.
Johnson, M. L., & Fraiser, S. G. (1985) *Methods Enzymol. 117*, 301–342.
Kawajima, K. (1989) *Proteins: Struct., Funct., Genet. 6*, 87–103.
Kim, P. S., & Baldwin, R. L. (1990) *Annu. Rev. Biochem. 59*, 631–660.
Lane, A. N., & Jardetzky, O. (1987) *Eur. J. Biochem. 164*, 389–396.
Mann, C. J., & Matthews, C. R. (1993) *Biochemistry 32*, 5282–5290.
Mann, C. J., Royer, C. A., & Matthews, C. R. (1993) *Protein Sci. 2*, 1853–1861.
Pace, C. N. (1986) *Methods Enzymol. 131*, 266–280.
Pace, C. N., Shirley, B. A., & Thomson, J. A. (1989) in *Protein Structure and Function: A Practical Approach* (Creighton, T. E., Ed.) pp 311–330, IRL Press, Oxford, England.
Pakula, A. A., & Sauer, R. T. (1989) *Proteins: Struct., Funct., Genet. 5*, 202–210.
Ptitsyn, O. B. (1987) *J. Protein Chem. 6*, 277–293.
Ramsay, G., & Eftink, M. R. (1994) *Biophys. J. 66*, 516–523.
Schellman, J. A. (1978) *Biopolymers 17*, 1305–1322.
Schevitz, R. W., Otwinowski, Z., Joachimiak, A., Lawson, C. L., & Sigler, P. B. (1985) *Nature 317*, 782–786.
Silva, J. L., Silveira, C. F., Correia, A., Jr., & Pontes, L. (1992) *J. Mol. Biol. 223*, 545–555.
Tasayco, M. L., & Carey, J. (1992) *Science 255*, 594–597.
Yang, J. T., Wu, C.-S. C., & Martinez, H. M. (1986) *Methods Enzymol. 130*, 208–269.
Zhang, R. G., Joachimiak, A., Lawson, C. L., Schevitz, R. W., Otwinowski, Z., & Sigler, P. B. (1987) *Nature 327*, 591–595.